CORTEX 120 (2019) 78–91

Available online at www.sciencedirect.com

ScienceDirect

Journal homepage: www.elsevier.com/locate/cortex

Research Report

Neural substrates of amodal and modality-specific semantic processing within the temporal lobe: A lesion-behavior mapping study of semantic dementia

Yan Chen [a,b,1], Keliang Chen [c,1], Junhua Ding [a], Yumei Zhang [d], Qing Yang [c], Yingru Lv [e], Qihao Guo [f] and Zaizhu Han [a,*]

[a] State Key Laboratory of Cognitive Neuroscience and Learning, IDG/McGovern Institute for Brain Research, Beijing Normal University, 100875, China
[b] College of Biomedical Engineering and Instrument Sciences, Zhejiang University, 310027, China
[c] Department of Neurology, Huashan Hospital, Fudan University, 200040, China
[d] Department of Radiology, Beijing Tiantan Hospital, Capital Medical University, 100050, China
[e] Department of Radiology, Huashan Hospital, Fudan University, 200040, China
[f] Department of Gerontology, Shanghai Jiaotong University Affiliated Sixth People's Hospital, 200233, China

ARTICLE INFO

Article history:
Received 29 July 2018
Reviewed 27 January 2019
Revised 27 March 2019
Accepted 29 May 2019
Action editor Peter Garrard
Published online 12 June 2019

Keywords:
Semantic memory
Amodal semantic hub
Modality-specific region
Temporal lobe
Lesion-behavior mapping analysis

ABSTRACT

Although the human temporal lobe has been documented to participate in semantic processing of both verbal and nonverbal stimuli, the exact neural basis underlying the common and unique processing of the two modalities is unclear. Semantic dementia (SD), a disease with a semantic-selective deficit due to predominant temporal lobe atrophy is an ideal lesion model to address this issue. However, many previous studies of SD used an impure patient sample or did not appropriately control for common components between tasks. To overcome these limitations, the present study aims to identify amodal semantic hubs and modality-specific regions in the temporal lobe by investigating behavioral performance on a verbal modality task (word associative matching) and a nonverbal modality task (picture associative matching) and neuroimaging data in 33 SD patients. We found that the left anterior fusiform gyrus was an amodal semantic hub whose gray matter volume correlated significantly with both modalities. We also observed two verbal modality-specific regions (the left posterior inferior temporal gyrus and the left middle superior temporal gyrus) and a nonverbal modality-specific region (the right lateral anterior middle temporal gyrus) whose gray matter volume correlated significantly with one modality when performance on the other modality was partialled out. The results remained significant when we excluded a wide range of potential confounding variables. Furthermore, to confirm the observed effects, we compared the performance of left- and right-hemispheric-predominant atrophic patients on the verbal and nonverbal tasks. The left-predominant patients showed more severe deficits in performance of the verbal task

* *Corresponding author.*
E-mail address: zzhhan@bnu.edu.cn (Z. Han).
[1] Yan Chen and Keliang Chen are co-first authors.
https://doi.org/10.1016/j.cortex.2019.05.014

than the right-predominant patients, whereas the two groups of patients presented comparable deficits in the performance of the nonverbal task. These findings refined the structure of semantic network in the temporal lobe, deepening our understanding of the critical role of the temporal lobe in semantic processing.

1. Introduction

The temporal lobe in the human brain has been found to be critical in semantic processing (Lambon Ralph, 2014; Rice, Lambon Ralph, & Hoffman, 2015; Vandenberghe, Price, Wise, Josephs, & Frackowiak, 1996). However, the exact basis of semantic processing of different types of information in the brain is not fully known (Gainotti, 2011, 2015; Lambon Ralph, Pobric, & Jefferies, 2009; Pobric, Jefferies, & Lambon Ralph, 2010). The specialization hypothesis speculates that left and right temporal lobes participate in information processing of verbal and nonverbal input modalities, respectively (Gainotti, 2011, 2012). However, the hub-and-spoke hypothesis proposes that temporal lobes serve as verbal and nonverbal spokes, and the anterior part of the temporal lobes (ATLs) underpins a semantic hub which unifies verbal and nonverbal conceptual knowledge to form a semantic concept (Lambon Ralph, 2014; Patterson, Nestor, & Rogers, 2007). Thus, one of the key scientific issues for semantic neural substrates is to precisely differentiate the brain areas of modality-specific and amodal semantic processing within the temporal lobe (Binney, Embleton, Jefferies, Parker, & Lambon Ralph, 2010; Lambon Ralph et al., 2009; Pobric, Jefferies, & Lambon Ralph, 2007; Visser & Lambon Ralph, 2011). Semantic dementia (SD) has been proven to be an ideal lesion model of semantic deficits to address this issue.

SD is a neurodegenerative disease associated with bilateral atrophy of the temporal lobes (Chan et al., 2001; Galton et al., 2001) and selective loss of semantic memory (Patterson et al., 2007). Patients with SD exhibit semantic impairments irrespective of input or output modalities, indicating the existence of an amodal semantic hub (Hoffman, Jones, & Lambon Ralph, 2012; Lambon Ralph, Sage, Jones, & Mayberry, 2010). Previous studies have indicated that the semantic hub is located in the temporal pole, and this is supported by studies involving functional neuroimaging (Price, Devlin, Moore, Morton, & Laird, 2005), and studies involving repetitive transcranial magnetic stimulation (rTMS; Pobric et al., 2010), as well as the localization of atrophy in SD patients (Butler, Brambati, Miller, & Gorno-Tempini, 2009; Patterson et al., 2007). Recent studies have begun to reveal that other regions, e.g., the left fusiform gyrus (FFG), act as an amodal semantic hub (Ding et al., 2016; Mion et al., 2010). For instance, Ding et al. (2016) found that the degree of atrophy of two temporal regions (the left FFG and the left parahippocampal gyrus) was associated with composite scores on verbal and nonverbal tasks in 19 SD patients. When the degree of atrophy of the other region was partialled out, only the left FFG maintained a significant correlation with the semantic composite scores on verbal and nonverbal tasks.

In addition to the evidence showing the existence of an ATL semantic hub, the existence of functional specialization between and within the temporal lobes based on input modalities has also been indicated in the literature (Gainotti, 2012, 2015; Rice, Caswell, Moore, Hoffman, & Lambon Ralph, 2018; Rice, Lambon Ralph et al., 2015). Evidence also comes from SD, in which temporal lobe atrophy is often asymmetric. Snowden, Thompson, and Neary (2004), for example, found that SD patients with left-predominant atrophy in ATL performed more poorly on tasks involving the recognition of famous people when the stimuli were presented as written names rather than as pictures. Patients with right-predominant atrophy in ATL showed the opposite pattern. Similar conclusions have been drawn based on studies using voxel-based morphometry to correlate behavioral performance on semantic tasks to gray matter integrity. For example, Butler et al. (2009) studied patients with neurodegenerative disease of mixed etiology and correlated performance on verbal and nonverbal versions of semantic association tasks with voxelwise gray matter atrophy. Stimuli modality-specific correlations were found in the left temporal regions for verbal stimuli and in the right fusiform gyrus for non-verbal stimuli. Acres, Taylor, Moss, Stamatakis, and Tyler (2009) examined a group of patients with temporal lobe damage due to SD, herpes simplex encephalitis and other causes, and found that integrity of the left inferior and anterior temporal regions was significantly correlated with verbal performance, whereas integrity of the right inferior and anterior temporal regions correlated with nonverbal performance.

Obviously, the above findings have provided important insights into amodal and modality-specific semantic regions in the temporal lobe. However, these findings should be interpreted with caution for the following reasons: 1) The participants in some of these studies included not only SD patients but also patients with other diseases, such as Alzheimer's disease, mild cognitive impairments (e.g., Butler et al., 2009) and herpes simplex encephalitis (e.g., Acres et al., 2009). Therefore, these findings required confirmation with a pure cohort of SD patients. 2) The identification of modality-specific regions might not have accurately considered the common components of verbal and nonverbal performance, such as selective attention and executive control (e.g., Acres et al., 2009). New studies should identify the modality-specific region when it is associated with the processing of a given modality even when the influence of the other modality is excluded. 3) The identification of amodal

hub semantic regions might be based on confounding behavioral measurements. For example, semantic ability in Ding et al. (2016) was measured with a semantic composite score that was calculated by combining verbal and nonverbal semantic performance. However, this measure might be driven by one of the modalities (e.g., verbal processing) due to its more severe deficits. Thus, the observed effects of amodal semantic regions might be associated only with the verbal or nonverbal modality but not with both modalities.

The present study aimed to identify amodal and modality-specific regions in the temporal lobe by considering the association and dissociation between verbal and nonverbal task performance in 33 SD patients. We calculated the correlation between the severity of verbal and nonverbal processing deficits and the degree of cortical atrophy across the patients. The severity of the deficits was measured by well-matched verbal (word) and nonverbal (picture) semantic associative matching tasks, and the atrophic degree was measured by determining the gray matter volume (GMV) of each voxel. The amodal semantic hub was identified by correlating voxelwise GMV with performance on the verbal and nonverbal tasks and then selecting the regions associated with both tasks. The modality-specific regions were identified by correlating voxelwise GMV with the patients' scores on one modality task (e.g., a verbal task), while partialling out the scores on the other modality task (a nonverbal task). To exclude the influence of primary visual perception, the performance on a perceptual matching control task was introduced as a covariate in all analyses. The results were further confirmed by statistically removing the effects of potential confounding variables (e.g., overall cognitive state, total GMV, and performance on two nonsemantic control tasks). Moreover, we also compared the performance on verbal and nonverbal tasks between the left- and right-predominant atrophic SD patients.

2. Materials and methods

2.1. Participants

SD patients and healthy control (HC) subjects were recruited from Huashan Hospital in Shanghai from 2011 to 2018. All participants were right-handed (Oldfield, 1971), native Chinese speakers and provided written informed consent. This study was approved by the Institutional Review Board of the Huashan Hospital affiliated with Fudan University.

SD patients. Thirty-three SD patients were included (15 males, age: 62.27 ± 7.49 years, educational level: 11.73 ± 3.01 years). Nineteen of them were from all of our recent study (Ding et al., 2016), and others were newly recruited. Each patient met the diagnostic criteria for SD (Gorno-Tempini et al., 2011) with the appearance of clinical diagnostic features (i.e., impaired confrontation naming, impaired single-word comprehension and predominant ATL atrophy) and at least three of other diagnostic features (i.e., impaired object knowledge particularly for low-frequency concepts, surface dyslexia, spared repetition and spared speech production). The neuropsychological tests and neuroimaging measures used for diagnosis can be found in Tables 1 and 2, respectively. The average score on the Mini-Mental State Examination (MMSE; Folstein, Folstein, & McHugh, 1975) was 21.91 ± 4.01.

Detailed procedures of our neuropsychological tests have been introduced in Ding et al. (2016). Here, we only described how we defined a Chinese speaker with surface dyslexia. We selected 24 Chinese semantic-phonetic compound characters. Each character contains a phonetic radical and a semantic radical that provide clues about the pronunciation and the meaning of the character, respectively (Bi, Han, Weekes, & Shu, 2007; Shu, Chen, Andersen, Wu, & Xuan, 2003; Weekes & Chen, 1999; Zhou & Marslen-Wilson, 1999). For example, the compound character "妈" (/mā/, mother) comprises the phonetic radical "马" (/mǎ/, horse) and the semantic radical "女" (/nǚ/, *female*). The compound characters consisted of 12 regular characters whose pronunciation are identical to those of their phonetic radicals (e.g., 蝗/huáng/grasshopper → phonetic radical: 皇/*huáng*/emperor; semantic radical: 虫/chóng/worm) and 12 irregular characters whose pronunciation differ from those of their phonetic radicals (烦/fán/annoyance → phonetic radical: 页/yè/emperor; semantic radical: 火/huǒ/anger). Each subject was instructed to read the 24 characters aloud. A patient was diagnosed with surface dyslexia if he or she, relative to healthy controls, presented an obvious regularity effect (i.e., reading accuracy for irregular characters was lower than that of regular ones) or a higher rate of regularization errors (i.e., an irregular word was misread as its phonetic radical; e.g., the word 烦 (/fán/) → 页/yè/). The cutoff values for the effects were set as lower than −1.96 for the corrected *t*-score of regularity effect (the correct numbers on irregular words minus those on regular words), or higher than 1.96 for the corrected *t*-score of regularization errors. The method obtaining the corrected *t*-score was explained in "Behavioral data preprocessing" section below.

Healthy controls. There were 20 HC subjects (8 males, age: 60.50 ± 3.93 years, educational level: 10.45 ± 2.89 years), who were identical to the healthy subjects of our recent study (Ding et al., 2016). Their MMSE score was 28.10 ± 1.37.

Compared with the HC group, the SD group was comparable in age, gender distribution, and educational level (p values > .05) but had a lower MMSE score ($t = -8.12$, $p < .001$).

2.2. Behavioral data collection

We carried out a series of neuropsychological assessments on SD and HC subjects using identical procedures (Table 1). Given that we were especially concerned with the association and dissociation between verbal and nonverbal semantic comprehension of patients, we mainly analyzed subjects' performance on word and picture associative matching tasks. In addition, a perceptual matching task was used to eliminate the influence of primary perceptual processing. Two nonsemantic control tasks (i.e., oral repetition and number calculation) that required minimal semantic processing were used to assess the semantic specificity of the observed regions. Participants were tested individually in a quiet room. Each task was run in separate sessions on a PC computer using the DMDX program (Forster & Forster, 2003). These tasks were used in our recent studies (Ding et al., 2016; Han et al., 2013; Zhao et al., 2017).

Table 1 – Demographic and neuropsychological profiles of SD patients and healthy controls.

Assessments	HC subjects (*n* = 20)	SD patients (n = 33)		Left-predominant SD patients (n = 16)		Right-predominant SD patients (n = 17)	
	Raw score	Raw score	Corrected *t*-score	Raw score	Corrected *t*-score	Raw score	Corrected *t*-score
Background information							
Age (years)	60.50 (3.93)	62.27 (7.49)		61.06 (7.89)		63.41 (7.14)	
Gender (M:F)	8:12	15:18		8:8		7:10	
Education (years)	10.45 (2.89)	11.73 (3.01)		12.13 (3.34)		11.35 (2.71)	
Neuropsychological tests used for diagnosis							
Confrontation naming							
Oral picture naming (n = 140)$^{\#}$	124.25 (7.95)	44.42 (26.60)***	−9.44 (3.26)	30.88 (22.93)***	−11.37 (2.88)	57.18 (23.79)***	−8.10 (2.93)
Oral sound naming (n = 36)$^{\#}$	25.40 (4.06)	8.39 (5.18)***	−3.85 (1.33)	8.44 (5.38)***	−3.89 (1.25)	8.35 (5.16)***	−3.81 (1.43)
Single-word comprehension							
Picture associative matching (n = 70)$^{+,\#}$	66.45 (2.39)	50.88 (6.77)***	−5.32 (2.36)	50.19 (8.63)***	−5.51 (3.04)	51.53 (4.56)***	−5.14 (1.56)
Word associative matching (n = 70)$^{+,\#}$	67.15 (1.46)	52.33 (8.34)***	−15.10 (9.11)	49.19 (9.12)***	−18.80 (9.92)	55.29 (6.48)***	−11.71 (6.90)
Word-picture verification (n = 70)$^{\#}$	67.25 (1.94)	42.36 (15.71)***	−11.40 (7.52)	38.00 (17.79)***	−13.50 (8.61)	46.47 (12.64)***	−9.41 (5.91)
Object knowledge for low-frequency concepts							
Naming to definition (n = 22)$^{+}$	18.35 (2.43)	5.06 (4.09)***	−7.81 (2.97)	2.69 (2.87)***	−8.98 (2.89)	7.44 (3.78)***	−6.64 (2.64)
Surface dyslexia							
Regularity effect of word reading (the correct numbers on irregular words – those on regular words)	−.40 (.82)	−2.12 (1.87)***	−2.35 (2.64)	−2.69 (2.09)**	−3.10 (3.03)	−1.59 (1.50)*	−1.65 (2.06)
Regularization errors of word reading (max = 12)	.40 (.75)	1.82 (1.42)***	2.69 (2.61)	2.13 (1.50)***	3.09 (2.79)	1.53 (1.53)**	2.32 (2.45)
Repetition							
Oral repetition (*n* = 12)$^{+}$	11.55 (.94)	11.39 (.83)*	−.84 (1.73)	11.31 (.95)	−1.05 (2.00)	11.47 (.72)	−.64 (1.46)
Speech production							
Percentage of reasonable sentences for Cookie Theft picture description (accuracy)	91% (13%)	90% (12%)	−.11 (.84)	90% (11%)	−.12 (.84)	90% (13%)	−.10 (.86)
Other neuropsychological tests							
Arithmetic ability							
Number calculation (*n* = 7)$^{+}$	6.50 (.69)	6.39 (.86)	−.27 (1.11)	6.63 (.62)	−.12 (.84)	6.18 (1.01)	−.52 (1.26)
Number proximity matching (*n* = 3)$^{\#}$	2.80 (.41)	2.61 (.66)	−.23 (1.43)	2.56 (.73)	−.38 (1.61)	2.65 (.61)	−.09 (1.28)
General cognitive state							
MMSE (max = 30)	27.95 (1.61)	21.91 (4.01)***	−3.90 (2.45)	21.69 (4.57)***	−4.06 (2.92)	22.12 (3.53)***	−3.74 (2.00)
Visual form perception							
Perceptual matching (*n* = 25)$^{+}$	23.95 (1.23)	21.91 (2.32)***	−2.23 (2.42)	21.50 (2.48)**	−2.52 (2.50)	22.29 (2.17)*	−1.96 (2.38)
Visual perception (*n* = 30)$^{\#}$	27.25 (1.62)	27.55 (1.80)	.13 (.86)	27.88 (1.50)	.29 (.69)	27.24 (2.05)	−.02 (.99)
Visuospatial perception							
REY-O copy (max = 36)	34.75 (1.77)	32.45 (3.86)*	−1.20 (1.72)	31.88 (4.94)	−1.42 (1.90)	33.00 (2.50)	−.99 (1.56)
Sound perception							
Sound perception (*n* = 44)$^{\#}$	38.55 (4.36)	33.42 (5.63)**	−.96 (1.02)	36.44 (4.50)	−.43 (.83)	30.59 (5.17)***	−1.45 (.95)
Episodic memory							
REY-O recall (max = 36)	16.05 (6.53)	9.33 (6.73)***	−1.35 (1.73)	9.31 (6.48)**	−1.46 (1.11)	9.35 (7.17)**	−1.24 (1.25)

Note: The values in table are mean (standard deviation). $^{+}$: the semantic and nonsemantic control tasks used in the main analysis; $^{\#}$: the semantic and nonsemantic tasks used in principal component analysis (PCA). *$p < .05$, **$p < .01$, ***$p < .001$ indicate significant difference with raw scores of healthy controls.

2.2.1. *Word associative matching*

This task was adapted from the Pyramids and Palm Trees test (Howard & Patterson, 1992). In each trial, the written names of three objects from the same category were simultaneously presented on the touch screen. Participants were instructed to decide which of the two bottom objects (e.g., axe, broom) was semantically closer to the top one (e.g., hammer). The response was made by pressing the corresponding object

Table 2 – Mean gray matter volume of the whole brain and ATLs in healthy controls, SD, left-predominant SD patients and right-predominant SD patients.

		In the whole brain (cm^3)	In the anterior temporal lobe (cm^3)		
			Left ATL	Right ATL	Left versus right ATL
Healthy subjects	Raw score	.39 (.03)	.50 (.05)	.50 (.05)	$p = .58$
All SD patients	Raw score	.35 (.05)***	.31 (.06)***	.31 (.10)***	$P = .92$
	Corrected *t*-score	−1.27 (1.17)	−3.15 (.99)	−3.54 (1.70)	$p = .28$
Left-predominant SD patients	Raw score	.36 (.05)*	.28 (.06)***	.39 (.09)***	$p < .0001$
	Corrected *t*-score	−1.02 (1.26)	−3.74 (.91)	−2.23 (1.39)	$p < .0001$
Right-predominant SD patients	Raw score	.34 (.04)***	.34 (.04)***	.24 (.04)***	$p < .0001$
	Corrected *t*-score	−1.50 (1.07)	−2.60 (.71)	−4.78 (.77)	$p < .0001$

Note: ATL = anterior temporal lobe. *$p < .05$, **$p < .01$, ***$p < .001$ indicate significant difference with raw scores of healthy controls.

name on the screen. There were 70 trials in total, in which 10 trials were from each of seven categories (i.e., animal, tool, common artifact, fruit and vegetable, large nonmanipulable object, person and action).

2.2.2. *Picture associative matching*

This task was identical to the word associative matching task except that the written names of objects were replaced with the corresponding pictures, and the item order was changed. Other behavioral tasks were inserted between these two matching tasks in order to reduce the practice effects.

2.2.3. *Perceptual matching*

We used the perceptual matching test from the Birmingham Object Recognition Battery ($n = 25$; Riddoch & Humphreys, 1993). In each trial, subjects were asked to decide which of the two bottom objects was viewed from a different perspective but had the same identity as the top object.

2.2.4. *Nonsemantic control tasks*

We designed two nonsemantic control tasks. The oral repetition task included eight words and four sentences. Participants were asked to repeat the words/sentences that they heard. The number calculation task included seven number calculation questions: two additions ($5 + 2$, $19 + 26$), two subtractions ($9 - 4$, $78 - 15$), two multiplications (2×4, 13×6), and one division ($6 \div 2$).

2.3. *Behavioral data preprocessing*

Because the patients who participated in this study varied considerably in demographic characteristics (e.g., age, gender, and education), their raw behavioral scores might not meaningfully reflect the degree of deficits. Our patients' behavioral scores were corrected by considering the performance distribution of the HC subjects and transforming each patient's raw score into a standardized *t*-score (Crawford & Garthwaite, 2006; see details in; Han et al., 2013). In brief, for each task, a regression model was first established in the HC group with raw accuracy scores as the dependent variable and age, gender and education as predictors. Then, a predicted accuracy for each patient was acquired by introducing his or her demographic information into the model. A discrepancy value was calculated with the following formula: $\text{Discrepancy}_{\text{patient}}$ = observed accuracy−predicted accuracy. Then, a corrected standard error of estimate for each patient ($SE_{patient}$) was obtained. Finally, the patient's *t*-score was computed: $t\text{-score}_{\text{patient}} = \text{Discrepancy}_{\text{patient}}/SE_{\text{patient}}$.

Moreover, we also obtained a measure of semantic ability that was unbiased for verbal and nonverbal processing. This measure was acquired from a principal component analysis (PCA) on basis of six general semantic tasks (oral picture naming, oral sound naming, picture associative matching, word associative matching, word-picture verification, and naming to definition) and three nonsemantic control tasks (visual perception, sound perception and number proximity matching). Specifically, the *t*-scores of the nine tasks were first entered into PCA program. We used subcommands for varimax rotation, plot of eigenvalues (>1), and principal components extraction. The semantic PCA factor was defined as a component that had a high loading weight on the semantic tasks but a low loading weight on the control tasks. The scores corresponding to this factor were considered to reflect semantic ability that was unbiased for verbal and nonverbal processing. These scores were used to confirm the amodal semantic region in the following validation analysis.

2.4. *Imaging data collection*

SD and HC subjects were scanned with a 3T Siemens scanner at Huashan Hospital in Shanghai. We obtained 3D T1-weighted MPRAGE images along the sagittal plane using the following parameters: repetition time (TR) = 2300 msec, echo time (TE) = 2.98 msec, flip angle = 9°, matrix size = 240 × 256, field of view (FOV) = 240 mm × 256 mm, slice number = 192 slices, slice thickness = 1 mm, and voxel size = 1 mm × 1 mm × 1 mm.

2.5. *Imaging data preprocessing*

T1 images were preprocessed using the VBM toolbox of the Statistical Parametric Mapping 8 (SPM8, http://www.fil.ion.ucl.ac.uk/spm/) software package with default parameters. T1-weighted images were segmented into gray matter (GM), white matter and cerebrospinal fluid at 1.5 mm × 1.5 mm × 1.5 mm resolution and normalized into the Montreal Neurological Institute (MNI) space using the Diffeomorphic Anatomical Registration Through Exponentiated Lie (DARTEL) registration method (Ashburner, 2007). The GM images were further modulated and smoothed with

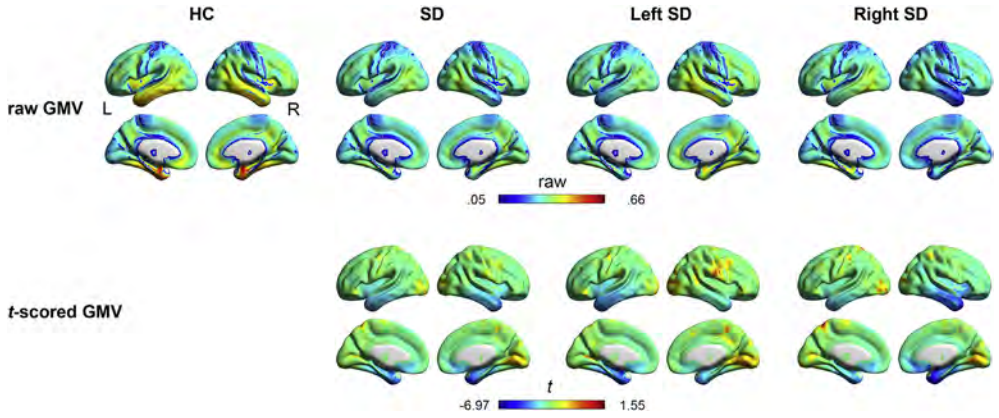

Fig. 1 – The mean gray matter volume (GMV) map of each subject group. The first row shows the mean of raw GMV images of healthy controls (HC), semantic dementia (SD) patients, left- and right-predominant atrophic SD patients. The second row shows the *t*-scored GMV maps of three patient groups obtained by considering the demographic variables and the GMV images of control subjects.

an 8-mm full-width at half maximum (FWHM) Gaussian kernel to obtain the gray matter volume (GMV) images. Since MRI with voxel-based morphometry can be insensitive in conditions of severe atrophy as occurs in SD (e.g., due to misregistration in severely atrophic regions), the main analyses were also carried out with 12-mm and 16-mm FWHM Gaussian kernels (Supplementary Figures 1 and 2).

The *t*-scored GMV images were generated for SD patients by considering three demographic variables (age, gender, and education) and GMV maps in reference healthy controls (Crawford & Garthwaite, 2006, Fig. 1). The method used to calculate the corrected *t*-score was identical to that in section "Behavioral data preprocessing". This analysis was conducted within a GM mask ($N_{voxels} = 278{,}516$), which was generated by thresholding the mean GM probability map of all 53 subjects with a cutoff value of .2 (Dai et al., 2014).

2.6. *Identification of amodal and modality-specific semantic regions*

To determine the cortical areas that are associated with amodal and modality-specific semantic processing, we conducted a lesion-behavior correlation analysis. Specifically, the amodal region was identified by overlapping the regions associated with both the verbal task and the nonverbal task. We computed the correlation between the GMV values of each voxel in the GM mask with the subject's performance on word associative matching and picture associative matching tasks, partialling out the scores on the perceptual matching task. The voxels that were significantly correlated with the performance of both tasks (AlphaSim-corrected $p < .001$; single voxel $p < .01$, cluster size > 745 voxels) were considered as the amodal semantic hub. The verbal and nonverbal modality-specific regions were identified by correlating the GMV values of each voxel within the GM mask with the scores on one semantic task (e.g., word associative matching) and partialling out the scores on the other semantic task (e.g., picture associative matching) and the perceptual matching control task (AlphaSim-corrected $p < .001$; single voxel $p < .01$, cluster size > 745 voxels).

2.7. *Validation of the effects of amodal and modality-specific semantic regions*

In the above main analysis, the amodal semantic hub was defined as the area of the overlap of the regions related to the verbal and nonverbal tasks. However, this analysis carried the risk that the effects of the so-called "hub" might be driven only by verbal or only by nonverbal semantic processing. To address this concern, a validated analysis was conducted by adopting another measure of semantic ability (i.e., semantic PCA factor) that was unbiased for verbal and nonverbal processing. The semantic PCA scores were correlated with the mean GMV of the hub region across SD patients, partialling out the demographic variables (age, gender and educational level).

Furthermore, to further determine whether the effects of the amodal and modality-specific regions that we observed in the above analyses were driven by other potential confounding variables, we applied a set of validation analyses. For each observed region in the above analyses, we again conducted partial correlation analysis between the mean GMV values of each semantic region and the semantic tasks while additionally controlling for the following variables: (1) the total GMV (summing the GMV values of all voxels in the whole brain), which was used to control for the overall severity of brain damage; (2) the MMSE score, which was used to control for overall cognitive state; (3) the oral repetition score, and (4) the number calculation score, which were both used to consider the influence of semantic specificity. Bonferroni correction $p < .05$ was adopted.

2.8. *Comparison of the verbal and nonverbal semantic performance in the left- and right-predominant-atrophic SD patients*

To further verify the laterality effects of ATLs in verbal and nonverbal processing, we divided our patients into left- and right-predominant-atrophic groups and compared the performances of the two groups on the verbal and nonverbal semantic tasks. The ATL regions were masked by adopting a

Table 3 – Amodal and modality-specific regions that were identified by calculating the correlations between the voxelwise gray matter volume (GMV) values and performance on the verbal and nonverbal semantic tasks across 33 SD patients.

Brain regions (AAL template)	Cluster size (voxels)	Peak coordinates MNI			r_{peak}
		x	y	z	
Amodal region					
Region A: Region correlated with word associative matching					
Cluster1: Left fusiform gyrus and left inferior temporal gyrus	9811	−39	−42	−18	.69***
left fusiform gyrus	2341				
left inferior temporal gyrus	2072				
Left middle temporal gyrus	1056				
left parahippocampus gyrus	730				
left middle temporal pole	609				
left superior temporal pole	545				
left superior temporal gyrus	453				
left insula	430				
left hippocampus gyrus	428				
Left amygdala	365				
Region B: Region correlated with picture associative matching					
Cluster1: Left anterior fusiform gyrus	788	−22.5	12	−37.5	.56***
left fusiform gyrus	132				
left amygdala	131				
left middle temporal pole	113				
left parahippocampus gyrus	109				
Amodal region: common region of region A and region B					
Cluster1: Left anterior fusiform gyrus	566				
left amygdala	130				
left fusiform gyrus	123				
left parahippocampus gyrus	109				
left middle temporal pole	79				
Verbal region: Region correlated with WAM scores partialling out PAM scores					
Cluster1: Left posterior inferior temporal gyrus	2151	−39	−42	−18	.64***
left fusiform gyrus	1428				
left inferior temporal gyrus	621				
Cluster2: Left middle superior temporal gyrus	2859	−57	−25.5	0	.62***
left middle temporal gyrus	1748				
left superior temporal gyrus	895				
Non-verbal region: Region correlated with PAM scores partialling out WAM scores					
Cluster1: Right anterior middle temporal gyrus	1604	58.5	10.5	−27	.55**
right middle temporal gyrus	1221				
right middle temporal pole	186				

Note: MNI = Montreal Neurological Institute; PAM = picture associative matching; WAM = word associative matching. *$p < .05$, **$p < .01$, ***$p < .001$.

previous method (Rice, Lambon Ralph et al., 2015; Supplementary Figure 3). The ATL included the areas anterior to the plane perpendicular to the long axis of the temporal lobe (passing through the fusiform gyrus at $y = -20$, $z = -30$ and superior temporal gyrus at $y = 0$, $z = -5$). A left-predominant-atrophic patient had a lower *t*-score of the mean GMV in the left ATL than those in the right ATL, vice versa. The two-way repeated-measures analysis of variance was conducted to analyze the effects of the 2 subject groups (the left-predominant atrophic SD *vs* right-predominant atrophic SD) and the 2 stimuli input modalities (nonverbal *vs* verbal) and their interaction.

3. Results

3.1. Clinical profiles of participants

The demographic and neuropsychological profiles of our subjects are shown in Table 1. The SD patients exhibited a profound impairment of semantic knowledge as indicated by severe deficits in confrontation naming (mean *t*-score < −6), single-word comprehension (mean *t*-score < −10), and object knowledge particularly for low-frequency concepts (mean *t*-score < −7). The patients also suffered from surface dyslexia with a regularity effect for reading words (mean *t*-score < −2) and considerable regularization errors (mean *t*-scores > 2). In contrast, the other cognitive abilities of the patients (e.g., repetition, speech production, arithmetic calculation, and episodic memory) were relatively spared (mean *t*-score > −1.35). The lower scores of the SD patients on the MMSE (mean *t*-score = −3.42) might arise from the semantic involvement of the test.

To evaluate whether the degree of semantic impairments of SD patients showed sufficient variation to meet the regression analysis standard, we examined the performance of our patients ($n = 33$) on the two key semantic task, each of which included 70 items. The mean accuracy of picture associative matching was 73% (*SD* = 10%; range: 53%–93%) and mean accuracy of the word associative matching was 75% (*SD* = 12%; range: 47%–96%). Furthermore, the patients'

accuracies on both tasks were significantly lower than those of healthy controls (*ps* < .001; see Table 1). These observations suggest that our group of patients included the individuals with mild to severe semantic dysfunction. Therefore, the data should be suitable for use in regression analyses.

Compared with HC subjects, SD subjects showed the most severe atrophy in the bilateral ATL, extending into the more posterior temporal lobes, insula and ventral frontal lobes (Fig. 1 and Table 2). Based on a comparison of the *t*-scores of the mean GMV of the left and right ATLs (Supplementary Figure 3), the SD patients could be divided into 16 left-predominant atrophic patients and 17 right-predominant patients. In all SD patients, the GMV values of the left and right ATLs were comparable (raw score: $p = .92$; *t*-score: $p = .28$; Table 2). In left-predominant SD patients, the GMV values of the left ATL were lower than those of the right ATL (raw score: $p < .0001$; *t*-score: $p < .0001$), while in right -predominant SD patients, the GMV values of the left ATL were higher than those of the right ATL (raw score: $p < .0001$; *t*-score: $p < .0001$; Table 2). The GMV values of the left ATL were lower in left-predominant SD patients than in right-predominant SD patients (raw score: $p < .001$; *t*-score: $p < .001$). Similarly, the values of the right ATL were lower in right-predominant SD patients than in left-predominant SD patients (raw score: $p < .0001$; *t*-score: $p < .0001$).

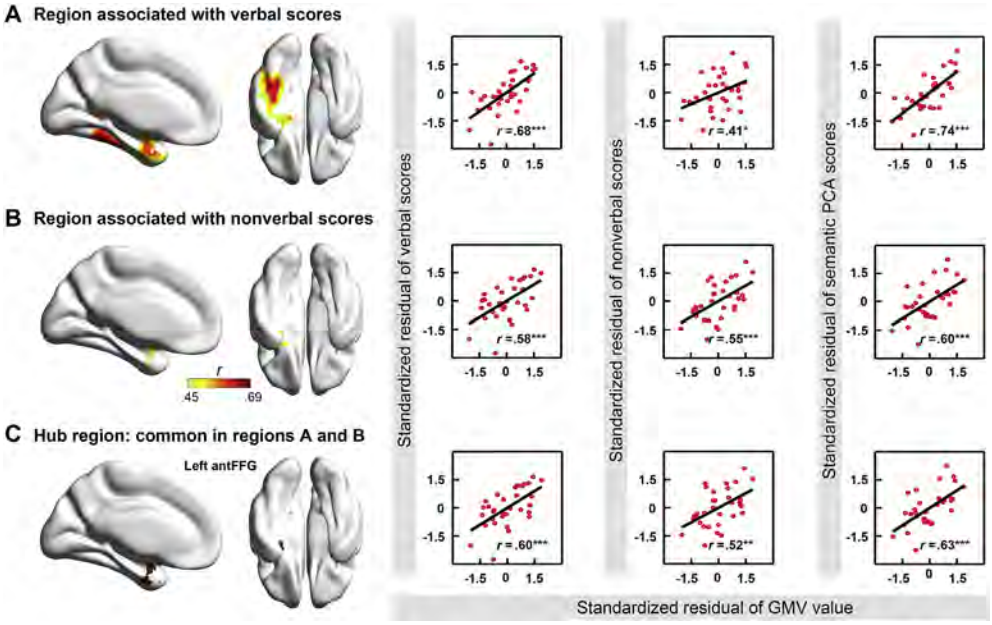

Fig. 2 – Amodal semantic region. We identified the amodal semantic region, the anterior fusiform gyrus (antFFG) (C), as a region that correlated significantly (AlphaSim-corrected $p < .001$) with the scores on both the word associative matching task (A) and the picture associative matching task (B). The scatter plots indicate the partial correlation between the mean GMV of the voxels within the cluster region with word associative matching, picture associative matching and semantic PCA scores after partialling out the scores on the perceptual matching test. The horizontal and vertical coordinates of the data are the residual of the GMV of the regions and the residual of the semantic tasks. *$p < .05$, **$p < .01$, ***$p < .001$.

3.2. *Amodal and modality-specific semantic regions*

The amodal and modality-specific regions that we observed are displayed in Table 3 and Figs. 2 and 3. To identify amodal semantic regions, we correlated the GMV values of each voxel with word associative matching and picture associative matching scores across 33 SD patients, partialling out the scores on the perceptual matching control task (AlphaSim-corrected $p < .001$). We found that GMV values of 9811 voxels were correlated with the verbal task, while GMV values of 788 voxels were correlated with the nonverbal task. These two analyses yielded a common cluster in the left anterior fusiform gyrus (antFFG; MNI coordinates of the center: −26.5, −6, −30; cluster size = 566 voxels).

To identify verbal-specific semantic regions, we correlated the GMV values of each voxel with scores on the verbal semantic task across SD patients, factoring out the scores on the nonverbal semantic task and the perceptual matching task (AlphaSim-corrected $p < .001$). We obtained two regions: the left posterior inferior temporal gyrus (posITG; peak coordinates: −39, −42, −18; peak partial $r = .64$, $p < .001$; cluster size = 2151 voxels) and the left middle superior temporal gyrus (midSTG; peak coordinates: −57, −25.5, 0; peak partial $r = .62$; peak $p < .001$; cluster size = 2859 voxels).

When identifying nonverbal semantic regions, we calculated the correlation between the GMV values of each voxel with the scores on the nonverbal semantic task across patients, factoring out the scores on the verbal semantic task and perceptual matching task (AlphaSim-corrected $p < .001$). We obtained one cluster in the right lateral anterior middle temporal gyrus (antMTG; peak coordinates: 58.5, 10.5, −27; peak partial $r = .55$; peak $p < .01$; cluster size = 1604 voxels).

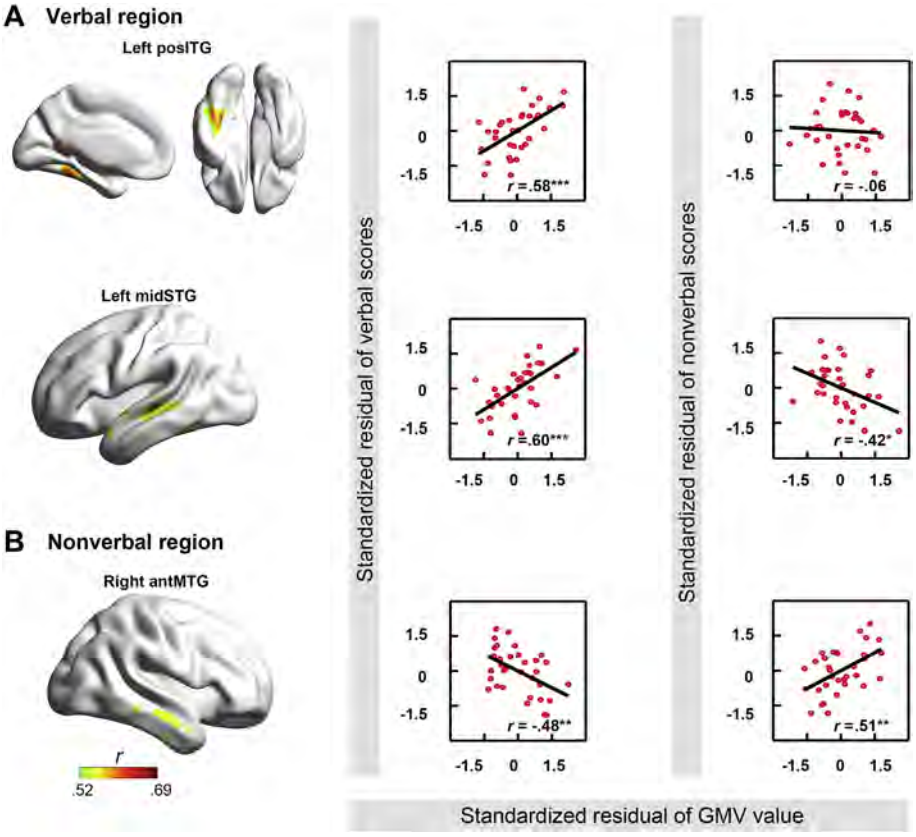

Fig. 3 – Modality-specific regions. (A) Verbal region: The GMVs of the left posterior inferior temporal gyrus (posITG) and the left middle superior temporal gyrus (midSTG) were significantly correlated with the scores on the verbal task (word associative matching) after controlling for scores on the nonverbal task (picture associative matching) and perceptual matching task (AlphaSim-corrected $p < .001$). (B) Nonverbal regions: The GMV of the right anterior middle temporal gyrus (antMTG) was significantly correlated (AlphaSim-corrected $p < .001$) with the scores on the nonverbal task after controlling for the scores on the verbal task and the perceptual matching task. The scatter plots show the partial correlation between the mean GMV within the cluster region with scores on the semantic task involving one modality after partialling out the scores on the perceptual matching test and the semantic task involving the other modality. $^{*}p < .05$, $^{**}p < .01$, $^{***}p < .001$.

When the GMV images were smoothed with larger FWHM Gaussian kernel (i.e., 12-mm and 16-mm), the result patterns were highly similar to those with the 8-mm kernel. The results of these two larger kernels were illustrated in Supplementary Figures 1 and 2.

3.3. *Validating the effects of the amodal and modality-specific semantic regions*

PCA analysis based on six general semantic tasks and three controls tasks extracted three components. Component 1

Table 4 – Partial correlation coefficients between the gray matter volume of the observed clusters and the semantic scores in SD patients, after additionally controlling for potential confounding factors (MMSE, total GMV, oral repetition, and number calculation).

Amodal and modality-specific regions	Behavior index	Partial correlation
Amodal region		
Left anterior fusiform gyrus	Correlated with WAM scores	.58**
	Correlated with PAM scores	.53*
	Correlated with semantic PCA scores	.61**
Verbal region		
Left posterior inferior temporal gyrus	Correlated with WAM scores partialling out PAM scores	.61**
Left middle superior temporal gyrus	Correlated with WAM scores partialling out PAM scores	.68***
Non-verbal region		
Right anterior middle temporal gyrus	Correlated with PAM scores partialling out WAM scores	.58**

Note: MMSE = Mini-Mental State Examination; PAM = picture associative matching; WAM = word associative matching. Bonferroni corrected: $^{*}p < .05$, $^{**}p < .01$, $^{***}p < .001$, i.e., $p < .0083$, $p < .0016$, $p < .00016$.

accounted for 46% of the model variance (under varimax rotation); the six general semantic tasks had higher loading values (.64–.74) and the three control tasks had lower loading values (−.09 to 0). We thus labeled this component as the semantic processing component and derived scores for each patient's general semantic processing ability based on this component. Components 2 (19% of model variance) and 3 (15% of model variance) were treated as perceptual and arithmetic components, respectively, because of their respective heaviest loading weights on the visual and auditory perceptual tasks (.79–.80) and on the number proximity matching task (.94). To eliminate the risk that the observed amodal region might be driven by verbal or nonverbal semantic processing, a validation analysis was conducted. We correlated the mean GMV value of the amodal region of the main result, i.e., the left antFFG, with the semantic PCA scores across the 33 SD patients, partialling out age, gender and educational level. The results demonstrated a significant correlation effect ($r = .65$, $p < .0001$), confirming that the amodal region we observed contributes to verbal and nonverbal semantic processing.

Table 4 shows the correlations between the GMV of the amodal or modality-specific semantic regions and the semantic scores of the patients after regressing out the influence of potential confounding factors. The mean GMV values of the amodal hub region, namely, the left antFFG, were still significantly correlated with all three semantic measures (verbal semantic score, nonverbal semantic score, semantic PCA score) when controlling for the MMSE scores, total gray matter volume, performance on the repetition task and calculation tasks (partial r values > .53, Bonferroni corrected p values < .05). Similarly, the effects of the modality-specific regions were still significant when the influence of potential confounding variables was eliminated (partial r values > .58, Bonferroni corrected p values < .01). These results demonstrate that the effects of the amodal and modality-specific regions could not be explained by the potential confounding variables.

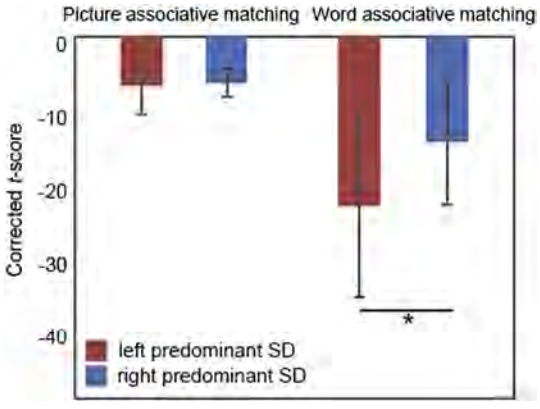

Fig. 4 – Behavioral performance on the verbal and nonverbal tasks by the left- and right-predominant atrophic SD patients. *$p < .05$.

3.4. *Distinctive performance on verbal and nonverbal tasks by the left- and right-predominant atrophic SD patients*

Fig. 4 shows the results of the two-factor repeated-measures analysis of variance of the 2 subject groups (the left-predominant atrophic SD patients *vs* right-predominant atrophic SD patients SD) and 2 stimuli input modalities (nonverbal *vs* verbal modalities). This analysis revealed a significant main effect of group ($F = 4.66$, $p = .039$), in which the left-predominant atrophic SD patients performed worse than the right-predominant atrophic SD patients on the two semantic tasks. We also observed a significant interaction between the two factors ($F = 6.48$, $p = .016$). A simple effect test indicated that the two SD groups exhibited comparable performance on the nonverbal task (i.e., the picture associative task) ($t = -.43$, $p = .67$), whereas the left-predominant atrophic SD subjects had lower scores on the verbal task (i.e., word associative matching) than the right-predominant atrophic SD subjects ($t = -2.40$, $p = .023$).

4. Discussion

The purpose of this study was to identify an amodal semantic hub and modality-specific regions in the temporal lobe using patients with SD as a lesion model. We attempted to overcome the shortcomings of previous studies by using a pure SD cohort and considering the association and dissociation between performance on the verbal and nonverbal tasks. By correlating the severity of deficits on the verbal and nonverbal tasks with the degree of cortical atrophy across of the 33 SD patients, we observed that the amodal semantic hub was located in the left antFFG. The verbal-specific regions included the left posITG and the midSTG, while the nonverbal-specific region included the right antMTG. These observed effects could not be accounted for by a wide range of potential confounding variables (e.g., MMSE score, total GMVs or performance on nonsemantic control tasks). We further found that the subjects with left-predominant atrophic SD performed more poorly on the verbal modality task than the subjects with right-predominant atrophic SD, but that the performance of the two groups on the nonverbal modality task was not significantly different. These observations provide new evidence for the existence of a semantic hub and reveal the location of amodal and modality-specific semantic regions within the temporal lobe (Patterson et al., 2007; Rogers et al., 2004).

4.1. *Left anterior fusiform gyrus: an amodal semantic hub region*

We found that the semantic hub was located in the left antFFG, consistent with the findings of other studies (Ding et al., 2016; Mion et al., 2010). Functional neuroimaging studies have also observed that the left antFFG engages in semantic processing during the performance of both verbal (Binder, Desai, Graves, & Conant, 2009; Binney et al., 2010;

Bright, Moss, & Tyler, 2004; Martin, 2007; Visser, Embleton, Jefferies, Parker, & Lambon Ralph, 2010) and nonverbal semantic tasks (Binney et al., 2010; Bright et al., 2004; Martin, 2007; Visser et al., 2010). This central hub integrates semantic verbal and nonverbal information and forms transmodal conceptual representations that capture deeper patterns of coherent variation across all sensory-motor and verbal modalities. Therefore, pathological changes in this area lead to both verbal and nonverbal semantic deficits in SD patients. We also observed that the left-predominant atrophic SD patients presented more severe semantic impairments than the right-predominant atrophic patients. This difference might also result from more severe damage to the left antFFG hub in the patients with left-predominant SD than in those with right-predominant SD.

Although we found that a large area of the left FFG is associated with semantic processing, only a very small part of it was found to represent the amodal semantic region (see Fig. 2). The roles of the areas beyond the amodal hub in semantic processing are unknown. Indeed, some researchers have proposed the "graded theory" to interpret the complex principle of semantic processing in the temporal lobe (Binney, Parker, & Lambon Ralph, 2012; Lambon Ralph, Jefferies, Patterson, & Rogers, 2016; Rice, Hoffman et al., 2015). This theory holds that the function of the semantic hub near the anterior basal temporal lobe is distinct from that of other regions due to its differential pattern of connectivity with other regions. Hub areas other than the amodal hub have advantages for specific functions. Thus, we speculate that the portion of the left FFG outside the amodal regions might be a graded hub area that not only contributes to all modalities but is also relatively specific to one given modality.

Notably, we found a role for the left antFFG but no role for the right antFFG in semantic processing. This finding is not consistent with the prominent hub-and-spoke theory, which argues that the semantic hub lies in both the left and right antFFG regions (Mion et al., 2010; Patterson et al., 2007). There might be three possible reasons for the null results for the right antFFG in our study. First, the right antFFG may also be a semantic hub, and the negative result might be due to our insensitive behavioral and imaging measures. Second, this region might be responsible for abstract semantic processing (Rice, Hoffman et al., 2015,Rice, Lambon Ralph et al., 2015); however, the use of concrete stimuli in the current study may have led to a failure to reveal significant effects. Finally, the region may not be a semantic hub, and the positive findings in previous studies might be driven by nonverbal semantic processes of this region.

4.2. *Hemispheric lateralization of verbal and nonverbal semantic processing*

We replicated previous research findings that showed that verbal and nonverbal modality-specific processes are supported by the left and right temporal lobes, respectively (Gainotti, 2012, 2015). The left verbal regions (posITG and midSTG) were found to be more strongly activated in verbal semantic tasks than in nonverbal tasks in functional studies (Thierry & Price, 2006; Vandenberghe et al., 1996). The left posITG might be engaged in orthographic lexical processing (Carreiras, Armstrong, Perea, & Frost, 2014), while the left midSTG is involved in phonological lexical retrieval (Binder et al., 2009; Graves, Grabowski, Mehta, & Gupta, 2008; Vigneau et al., 2006). By linking verbal input with semantic content, these regions support verbal information comprehension. Nonverbal effects of the right region (antMTG) were also reported in SD patients (Butler et al., 2009). Furthermore, functional neuroimaging studies have also observed enhanced activation in response to nonverbal stimuli in the region (Tsukiura, Mochizuki-Kawai, & Fujii, 2006). These observations support the view that a visual object is perceived in the primary visual cortices and that the visual information is then transferred to the temporal lobe via the inferior longitudinal fasciculus. In the anterior temporal lobe, the visual attributes of the object are further processed, and the object is recognized (Behrmann & Plaut, 2015).

We further observed a significant interaction between cerebral atrophy laterality and stimuli input modality. Left- and right-predominant atrophic SD patients performed comparably on the nonverbal task (picture associative matching). This comparable performance might have occurred because the two subject groups exhibited damage in the left hub and the right nonverbal regions, respectively. These two types of brain regions both participate in nonverbal processing. In contrast, the left-predominant atrophic SD patients displayed more severe impairment on the verbal task (word associative matching task) than did the right-predominant patients. This difference might be interpreted as indicating that there was greater damage to the left verbal-specific regions in the left-predominant patients than in the right-predominant patients.

The current study and previous studies which compared left and right SD patients consistently revealed marked dissociations of verbal deficits (impairments on naming or word-based semantic tests) and nonverbal deficits (impairments on picture-based semantic tests) in the two subgroups (Binney et al., 2016; Snowden et al., 2018, 2004; Woollams & Patterson, 2018). This hemispheric lateralization of verbal and nonverbal semantic processing indicated by these SD studies was reinforced by the results found in other brain-injured individuals, such as patients with postsurgical temporal lobe epilepsy (TLE). Left-resected TLE patients showed weaker performance on tasks that required accessing semantic information from a written word, whereas right-resected TLE patients were relatively more impaired at recognizing information from pictures (Rice et al., 2018). Moreover, the results are also consistent with rTMS studies (Woollams, Lindley, Pobric, & Hoffman, 2017) and functional MRI in healthy participants (Rice, Lambon Ralph et al., 2015). The specialization of the left and right ATLs might arise from differential functional and structural connectivity with language regions and perceptual regions (Lambon Ralph et al., 2016; Lambon Ralph, McClelland, Patterson, Galton, & Hodges, 2001; Pobric et al., 2010).

4.3. *Bilateral pattern of atrophy of two hemispheres in SD patients*

The 33 SD patients in the current study showed a bilaterally balanced atrophy between the left and right ATLs (see Table 2, Fig. 1). This pattern is rarely reported in the literature. Most

previous studies found more left-lateralized severe degeneration in SD patients. Our results might be because we recruited similar numbers of patients with left- and right-predominant atrophy (16 *vs* 17). When these two types of patients were considered as a single group, no difference in atrophy between the ATLs in the two hemisphers was observed. In contrast, most previous studies have included more individuals with left-than right-predominant atrophy (e.g., 70 *vs* 24, Hodges et al., 2010; 36 *vs* 11, Thompson, Patterson, & Hodges, 2003; 10 *vs* 3, Snowden et al., 2004; 6 *vs* 0, Mummery et al., 2000; 5 *vs* 0, Hodges & Patterson, 1996). Thus, these previous studies observed a left-predominant atrophy pattern in SD. It is noteworthy that an elegant study by Mion et al. (2010) selected the same numbers of left- and right-predominant atrophy SD patients (15 *vs* 15), and compared their behavioral performance. We surmise that the effects of the laterality of cortical atrophy might become less significant when the patients are assessed as a single group.

4.4. *Limitations*

This study has some caveats. First, the neuropathological profiles of the SD patients were not assessed, although the patients' clinical data were collected. Second, we only identified amodal and modality-specific regions for the visual modality; thus, whether the effects of these regions could also be generalized to other modalities (e.g., auditory, tactile) is unclear. Third, we administered the word and picture associative tasks in a fixed order. A practice effect or fatigue effect might have occurred because the picture tasks was always performed after the word task. Future studies should balance the testing order among subjects. Finally, the hub-and-spoke theory speculates that information is interchanged between the semantic hub and modality-specific regions. The current study only identified these local brain regions. In the future, we should further reconstruct the functional and structural connectivity between the regions.

4.5. *Conclusion*

By investigating the relationship between the GMV values and semantic verbal and nonverbal performance, we identified the semantic hub and modality-specific regions in the temporal lobe. We observed that the verbal information associated with an object is represented in the left posITG and left midSTG, while the nonverbal information associated with the object is represented in the right antMTG. Eventually, these pieces of modality-specific information converge in the hub region (i.e., the left antFFG) to achieve conceptual recognition. These results provide new evidence for the organization of semantic memory on the basis of the SD lesion model, deepening our understanding of the neuroanatomical network of semantic processing.

Declarations of interest

None.

CRediT authorship contribution statement

Yan Chen: Conceptualization, Software, Formal analysis, Writing - original draft, Writing - review & editing. **Keliang Chen:** Data curation, Software, Formal analysis, Writing - review & editing. **Junhua Ding:** Software, Formal analysis. **Yumei Zhang:** Methodology. **Qing Yang:** Data curation. **Yingru Lv:** Data curation. **Qihao Guo:** Methodology, Resources. **Zaizhu Han:** Conceptualization, Methodology, Writing - review & editing, Supervision, Funding acquisition.

Acknowledgements

We would like to thank all research participants for their patience. This work was supported by the National Key R&D Program of China (2018YFC1315200), China, the National Natural Science Foundation of China (81171019), China and the Beijing Natural Science Foundation (7182088), China.

Supplementary data

Supplementary data to this article can be found online at https://doi.org/10.1016/j.cortex.2019.05.014.

REFERENCES

Acres, K., Taylor, K. I., Moss, H. E., Stamatakis, E. A., & Tyler, L. K. (2009). Complementary hemispheric asymmetries in object naming and recognition: A voxel-based correlational study. *Neuropsychologia, 47*, 1836–1843. https://doi.org/10.1016/j.neuropsychologia.2009.02.024.

Ashburner, J. (2007). A fast diffeomorphic image registration algorithm. *Neuroimage, 38*, 95–113. https://doi.org/10.1016/j.neuroimage.2007.07.007.

Behrmann, M., & Plaut, D. C. (2015). A vision of graded hemispheric specialization. *Annals of the New York Academy of Sciences, 1359*, 30–46. https://doi.org/10.1111/nyas.12833.

Bi, Y., Han, Z., Weekes, B., & Shu, H. (2007). The interaction between semantic and the nonsemantic systems in reading: Evidence from Chinese. *Neuropsychologia, 45*, 2660–2673. https://doi.org/10.1016/j.neuropsychologia.2007.02.007.

Binder, J. R., Desai, R. H., Graves, W. W., & Conant, L. L. (2009). Where is the semantic system? A critical review and meta-analysis of 120 functional neuroimaging studies. *Cerebral Cortex, 19*, 2767–2796. https://doi.org/10.1093/cercor/bhp055.

Binney, R. J., Embleton, K. V., Jefferies, E., Parker, G. J. M., & Lambon Ralph, M. A. (2010). The ventral and inferolateral aspects of the anterior temporal lobe are crucial in semantic memory: Evidence from a novel direct comparison of distortion-corrected fMRI, rTMS, and semantic dementia. *Cerebral Cortex, 20*, 2728–2738. https://doi.org/10.1093/cercor/bhq019.

Binney, R. J., Henry, M. L., Babiak, M., Pressman, P. S., Santos-Santos, M. A., Narvid, J., et al. (2016). Reading words and other people: A comparison of exception word, familiar face and affect processing in the left and right temporal variants of primary progressive aphasia. *Cortex, 82*, 147–163. https://doi.org/10.1016/j.cortex.2016.05.014.

Binney, R. J., Parker, G. J. M., & Lambon Ralph, M. A. (2012). Convergent connectivity and graded specialization in the rostral human temporal lobe as revealed by diffusion-weighted imaging probabilistic tractography. *Journal of Cognitive Neuroscience, 24*, 1998–2014. https://doi.org/10.1162/jocn_a_00263.

Bright, P., Moss, H., & Tyler, L. K. (2004). Unitary vs multiple semantics: PET studies of word and picture processing. *Brain and Language, 89*, 417–432. https://doi.org/10.1016/j.bandl.2004.01.010.

Butler, C. R., Brambati, S. M., Miller, B. L., & Gorno-Tempini, M. L. (2009). The neural correlates of verbal and non-verbal semantic processing deficits in neurodegenerative disease. *Cognitive and Behavioral Neurology: Official Journal of the Society for Behavioral and Cognitive Neurology, 22*, 73–80. http://doi.org/10.1097/WNN.0b013e318197925d.

Carreiras, M., Armstrong, B. C., Perea, M., & Frost, R. (2014). The what, when, where, and how of visual word recognition. *Trends in Cognitive Sciences, 18*, 90–98. https://doi.org/10.1016/j.tics.2013.11.005.

Chan, D., Fox, N. C., Scahill, R. I., Crum, W. R., Whitwell, J. L., Leschziner, G., et al. (2001). Patterns of temporal lobe atrophy in semantic dementia and Alzheimer's disease. *Annals of Neurology, 49*(4), 433–442. https://doi.org/10.1002/ana.92.

Crawford, J. R., & Garthwaite, P. H. (2006). Comparing patients' predicted test scores from a regression equation with their obtained scores: A significance test and point estimate of abnormality with accompanying confidence limits. *Neuropsychology, 20*(3), 259. https://doi.org/10.1037/0894-4105.20.3.259.

Dai, Z., Yan, C., Li, K., Wang, Z., Wang, J., Cao, M., et al. (2014). Identifying and mapping connectivity patterns of brain network hubs in Alzheimer's disease. *Cerebral Cortex, 25*, 1–20. https://doi.org/10.1093/cercor/bhu246.

Ding, J., Chen, K., Chen, Y., Fang, Y., Yang, Q., Lv, Y., et al. (2016). The left fusiform gyrus is a critical region contributing to the core behavioral profile of semantic dementia. *Frontiers in Human Neuroscience, 10*, 215. https://doi.org/10.3139/fnhum.2016.00215.

Folstein, M. F., Folstein, S. E., & McHugh, P. R. (1975). "Mini-mental state": A practical method for grading the cognitive state of patients for the clinician. *Journal of Psychiatric Research, 12*(3), 189–198. https://doi.org/10.1016/0022-3956(75)90026-6.

Forster, K. I., & Forster, J. C. (2003). DMDX: A windows display program with millisecond accuracy. *Behavior Research Methods, Instruments, & Computers, 35*(1), 116–124. https://doi.org/10.33758/BF03195503.

Gainotti, G. (2011). The organization and dissolution of semantic-conceptual knowledge: Is the 'amodal hub' the only plausible model? *Brain and Cognition, 75*(3), 299–309. https://doi.org/10.1016/j.bandc.2010.12.001.

Gainotti, G. (2012). The format of conceptual representations disrupted in semantic dementia: A position paper. *Cortex, 48*(5), 521–529. https://doi.org/10.1016/j.cortex.2011.06.019.

Gainotti, G. (2015). Is the difference between right and left ATLs due to the distinction between general and social cognition or between verbal and non-verbal representations? *Neuroscience and Biobehavioral Reviews, 51*, 296–312. https://doi.org/10.1016/j.neubiorev.2015.02.004.

Galton, C. J., Patterson, K., Graham, K., Lambon Ralph, M. A., Williams, G., Antoun, N., et al. (2001). Differing patterns of temporal atrophy in Alzheimer's disease and semantic dementia. *Neurology, 57*(2), 216–225. https://doi.org/10.1212/WNL.57.2.216.

Gorno-Tempini, M. L., Hillis, A. E., Weintraub, S., Kertesz, A., Mendez, M., Cappa, S. F., et al. (2011). Classification of primary progressive aphasia and its variants. *Neurology, 76*(11), 1006–1014. https://doi.org/10.1212/WNL.0b013e31821103e6.

Graves, W. W., Grabowski, T. J., Mehta, S., & Gupta, P. (2008). The left posterior superior temporal gyrus participates specifically in accessing lexical phonology. *Journal of Cognitive Neuroscience, 20*(9), 1698–1710. https://doi.org/10.1162/jocn.2008.20113.

Han, Z., Ma, Y., Gong, G., He, Y., Caramazza, A., & Bi, Y. (2013). White matter structural connectivity underlying semantic processing: Evidence from brain damaged patients. *Brain, 136*, 2952–2965. https://doi.org/10.1093/brain/awt205.

Hodges, J. R., Mitchell, J., Dawson, K., Spillantini, M. G., Xuereb, J. H., McMonagle, P., et al. (2010). Semantic dementia: Demography, familial factors and survival in a consecutive series of 100 cases. *Brain, 133*(1), 300–306. https://doi.org/10.1093/brain/awp248.

Hodges, J. R., & Patterson, K. (1996). Nonfluent progressive aphasia and semantic dementia: A comparative neuropsychological study. *Journal of the International Neuropsychological Society, 2*(6), 511–524. https://doi.org/10.1017/s1355617700001685.

Hoffman, P., Jones, R. W., & Lambon Ralph, M. A. (2012). The degraded concept representation system in semantic dementia: Damage to pan-modal hub, then visual spoke. *Brain, 135*(12), 3770–3780. https://doi.org/10.1093/brain/aws282.

Howard, D., & Patterson, K. (1992). *Pyramids and palm trees test: Access from words and pictures*. Bury St Edmunds (UK): Thames Valley Test Company.

Lambon Ralph, M. A. (2014). Neurocognitive insights on conceptual knowledge and its breakdown. *Philosophical Transactions of the Royal Society B-Biological Sciences, 369*(1634), 2012392. https://doi.org/10.1098/rstb.2012.0392.

Lambon Ralph, M. A., Jefferies, E., Patterson, K., & Rogers, T. T. (2016). The neural and computational bases of semantic cognition. *Nature Reviews Neuroscience, 18*, 42–55. https://doi.org/10.1038/nrn.2016.150.

Lambon Ralph, M. A., McClelland, J. L., Patterson, K., Galton, C. J., & Hodges, J. R. (2001). No right to speak? The relationship between object naming and semantic impairment: Neuropsychological evidence and a computational model. *Journal of Cognitive Neuroscience, 13*(3), 341–356. https://doi.org/10.1162/08989290151137395.

Lambon Ralph, M. A., Pobric, G., & Jefferies, E. (2009). Conceptual knowledge is underpinned by the temporal Pole bilaterally: Convergent evidence from rTMS. *Cerebral Cortex, 19*(4), 832–838. https://doi.org/10.1093/cercor/bhn131.

Lambon Ralph, M. A., Sage, K., Jones, R. W., & Mayberry, E. J. (2010). Coherent concepts are computed in the anterior temporal lobes. *Proceedings of the National Academy of Sciences of the United States of America, 107*(6), 2717–2722. https://doi.org/10.1073/pnas.0907307107.

Martin, A. (2007). The representation of object concepts in the brain. *Annual Review of Psychology, 58*, 25–45. https://doi.org/10.1146/annurev.psych.57.102904.190143.

Mion, M., Patterson, K., Acosta-Cabronero, J., Pengas, G., Izquierdo-Garcia, D., Hong, Y. T., et al. (2010). What the left and right anterior fusiform gyri tell us about semantic memory. *Brain, 133*(11), 3256–3268. https://doi.org/10.1093/brain/awq272.

Mummery, C. J., Patterson, K., Price, C. J., Ashburner, J., Frackowiak, R. S. J., & Hodges, J. R. (2000). A voxel-based morphometry study of semantic dementia: Relationship between temporal lobe atrophy and semantic memory. *Annals of Neurology, 47*(1), 36–45. https://doi.org/10.1002/1531-8249(200001)47:1<36::AID-ANA8>3.0.CO;2-L.

Oldfield, R. C. (1971). The assessment and analysis of handedness: The Edinburgh inventory. *Neuropsychologia, 9*(1), 97–113. https://doi.org/10.1016/0028-3932(71)90067-4.

Patterson, K., Nestor, P. J., & Rogers, T. T. (2007). Where do you know what you know? The representation of semantic

knowledge in the human brain. *Nature Reviews Neuroscience, 8*(12), 976–987. https://doi.org/10.1038/nrn2277.

Pobric, G., Jefferies, E., & Lambon Ralph, M. A. (2007). Anterior temporal lobes mediate semantic representation: Mimicking semantic dementia by using rTMS in normal participants. *Proceedings of the National Academy of Sciences of the United States of America, 104*(50), 20137–20141. https://doi.org/10.1073/pnas.0707383104.

Pobric, G., Jefferies, E., & Lambon Ralph, M. A. (2010). Amodal semantic representations depend on both anterior temporal lobes: Evidence from repetitive transcranial magnetic stimulation. *Neuropsychologia, 48*(5), 1336–1342. https://doi.org/10.1016/j.neuropsychologia.2009.12.036.

Price, C. J., Devlin, J. T., Moore, C. J., Morton, C., & Laird, A. R. (2005). Meta-analyses of object naming: Effect of baseline. *Human Brain Mapping, 25*(1), 70–82. https://doi.org/10.1002/hbm.20132.

Rice, G. E., Caswell, H., Moore, P., Hoffman, P., & Lambon Ralph, M. A. (2018). The roles of left versus right anterior temporal lobes in semantic memory: A neuropsychological comparison of postsurgical temporal lobe epilepsy patients. *Cerebral Cortex, 28*(4), 1487–1501. https://doi.org/10.1093/cercor/bhx362.

Rice, G. E., Hoffman, P., & Lambon Ralph, M. A. (2015). Graded specialization within and between the anterior temporal lobes. *Annals of the New York Academy of Sciences, 1359*, 84–97. https://doi.org/10.1111/nyas.12951.

Rice, G. E., Lambon Ralph, M. A., & Hoffman, P. (2015). The roles of left versus right anterior temporal lobes in conceptual knowledge: An ALE meta-analysis of 97 functional neuroimaging studies. *Cerebral Cortex, 25*(11), 4374–4391. https://doi.org/10.1093/cercor/bhv024.

Riddoch, M. J., & Humphreys, G. W. (1993). *BORB: Birmingham object recognition Battery*. UK: Lawrence Erlbaum Associates Ltd.

Rogers, T. T., Lambon Ralph, M. A., Garrard, P., Bozeat, S., McClelland, J. L., Hodges, J. R., et al. (2004). Structure and deterioration of semantic memory: A neuropsychological and computational investigation. *Psychological Review, 111*(1), 205–235. https://doi.org/10.1037/0033-295X.111.1.205.

Shu, H., Chen, X., Andersen, R. C., Wu, N., & Xuan, Y. (2003). Properties of School Chinese: Implications for learning to read. *Child Development, 74*(1), 27–47. https://doi.org/10.1111/1467-8624.00519.

Snowden, J. S., Harris, J. M., Thompson, J. C., Kobylecki, C., Jones, M., Richardson, A. M., et al. (2018). Semantic dementia and the left and right temporal lobes. *Cortex, 107*, 188–203. https://doi.org/10.1016/j.cortex.2017.08.024.

Snowden, J. S., Thompson, J. C., & Neary, D. (2004). Knowledge of famous faces and names in semantic dementia. *Brain, 127*(4), 860–872. https://doi.org/10.1093/brain/awh099.

Thierry, G., & Price, C. J. (2006). Dissociating verbal and nonverbal conceptual processing in the human brain. *Journal of Cognitive Neuroscience, 18*, 1018–1028. https://doi.org/10.1162/jocn.2006.18.6.1018.

Thompson, S. A., Patterson, K., & Hodges, J. R. (2003). Left/right asymmetry of atrophy in semantic dementia: Behavioral-cognitive implications. *Neurology, 61*(9), 1196–1203. https://doi.org/10.1212/01.WNL.0000091868.28557.B8.

Tsukiura, T., Mochizuki-Kawai, H., & Fujii, T. (2006). Dissociable roles of the bilateral anterior temporal lobe in face-name associations: An event-related fMRI study. *Neuroimage, 30*(2), 617–626. https://doi.org/10.1016/j.neuroimage.2005.09.043.

Vandenberghe, R., Price, C., Wise, R., Josephs, O., & Frackowiak, R. S. (1996). Functional anatomy of a common semantic system for words and pictures. *Nature, 383*(6597), 254–256. https://doi.org/10.1038/38254a0.

Vigneau, M., Beaucousin, V., Hervé, P. Y., Duffau, H., Crivello, F., Houdé, O., et al. (2006). Meta-analyzing left hemisphere language areas: Phonology, semantics, and sentence processing. *Neuroimage, 30*(4), 1414–1432. https://doi.org/10.1016/j.neuroimage.2005.11.002.

Visser, M., Embleton, K. V., Jefferies, E., Parker, G. J., & Lambon Ralph, M. A. (2010). The inferior, anterior temporal lobes and semantic memory clarified: Novel evidence from distortion-corrected fMRI. *Neuropsychologia, 48*(6), 1689–1696. https://doi.org/10.1016/j.neuropsychologia.2010.02.016.

Visser, M., & Lambon Ralph, M. A. (2011). Differential contributions of bilateral ventral anterior temporal lobe and left anterior superior temporal gyrus to semantic processes. *Journal of Cognitive Neuroscience, 23*(10), 3121–3131. https://doi.org/10.1162/jocn_a_00007.

Weekes, B., & Chen, H. (1999). Surface dyslexia in Chinese. *Neurocase, 5*, 161–172. https://doi.org/10.1080/13554799908415480.

Woollams, A. M., Lindley, J. L., Pobric, G., & Hoffman, P. (2017). Laterality of anterior temporal lobe repetitive transcranial magnetic stimulation determines the degree of disruption in picture naming. *Brain Structure & Function, 222*(8), 3749–3759. https://doi.org/10.1007/s00429-017-1430-2.

Woollams, A. M., & Patterson, K. (2018). Cognitive consequences of the left-right asymmetry of atrophy in semantic dementia. *Cortex, 107*, 64–77. https://doi.org/10.1016/j.cortex.2017.11.014.

Zhao, Y., Song, L., Ding, J., Lin, N., Wang, Q., Du, X., et al. (2017). Left anterior temporal lobe and bilateral anterior cingulate cortex are semantic hub regions: Evidence from behavior-nodal degree mapping in brain-damaged patients. *Journal of Neuroscience, 37*(1), 141–151. https://doi.org/10.1523/JNEUROSCI.1946-16.2017.

Zhou, X., & Marslen-Wilson, W. (1999). The nature of sublexical processing in reading Chinese characters. *Journal of Experimental Psychology: Learning, Memory, and Cognition, 25*(4), 819–837. https://doi.org/10.1037/0278-7393.25.4.819.